

# Synthesis and Characterization of Transition Metal Complexes of Mono Thiourea as Ligand and its Nonlinear Optic Application

Syaziemah Jasmani<sup>a</sup>, Mamoona Jillani<sup>a</sup>, Suhaila Sapari<sup>a</sup>, Fazira Ilyana Abdul Razak<sup>\*a</sup>

<sup>a</sup> Department of Chemistry, Faculty of Science, Universiti Teknologi Malaysia, 81310 UTM Johor Bahru, Johor, Malaysia.

## Article history

Received

5 November 2024

Revised

27 November 2024

Accepted

29 November 2024

Published online

30 November 2024

\*Corresponding author  
faziraillyana@utm.my

## Abstract

1,3-Diphenylthiourea (DPTU) is a promising candidate as a nonlinear optical (NLO) material due to its electronic structure, high dipole moment, and potential for strong nonlinear optical responses. It could be used in various photonic applications such as laser frequency conversion, optical switching, and signal processing. This study investigates the nonlinear optics (NLO) properties of metal complexes formed by using 1,3-diphenylthiourea as a ligand with different transition metals (copper, cadmium, and cobalt, labeled CA, CB, and CC respectively). Ligand was synthesized with a 70% yield. The characterization was performed using Fourier Transform Infrared (FT-IR), Nuclear Magnetic Resonance (NMR), and Ultraviolet-Visible (UV-Vis) spectroscopy. Density Functional Theory (DFT) calculations with the 6-31G (d,p) basis set at the B3LYP level were used to optimize the structure of thiourea and compute the IR, <sup>1</sup>H NMR, and UV-Vis spectra, which were then validated against experimental data. FT-IR analysis showed the C=S stretching peak at 1242.98 cm<sup>-1</sup> (experimental) and 1200.34 cm<sup>-1</sup> (computational) for the ligand. Upon complexation, the C=S stretching frequencies shifted to 1028.01 cm<sup>-1</sup> (CA), 1183.81 cm<sup>-1</sup> (CB), and 1205.50 cm<sup>-1</sup> (CC) experimentally, and to 1035.74 cm<sup>-1</sup> (CA), 1196.70 cm<sup>-1</sup> (CB), and 1221.18 cm<sup>-1</sup> (CC) computationally, with deviations under 5%. NMR analysis revealed amine peak signals at δ 9.633 ppm (H, NHa) and δ 8.169 ppm (H, NHb) for the ligand, shifting to δ 8.621 ppm (H, NHa) and δ 7.402 ppm (H, NHb) for CA. UV-Vis spectroscopy showed a π-π\* transition for the ligand at 238 nm, shifting to 253 nm (CA), 266 nm (CB), and 265 nm (CC), with additional Metal-to-Ligand Charge Transfer (MLCT) transitions at 701 nm (CA), 429 nm (CB), and 507 nm (CC). DFT calculations indicated that the cobalt complex (CC) exhibits the highest NLO properties, with a frequency-dependent first hyperpolarizability (β<sub>tot</sub>) value of 6030.985 × 10<sup>-30</sup> esu at 1064 nm, supported by a high dipole moment and low energy gap, making it the best candidate for NLO applications.

**Keywords** Thiourea; ligand; metal complexes; DFT; NLO

© 2024 Penerbit UTM Press. All rights reserved

## 1.0 INTRODUCTION

Nonlinear optical (NLO) materials are crucial for applications in signal processing, data storage, sensing, and optoelectronics. These materials, including switchable molecular systems, have significantly contributed to advancements in nanotechnology. Enhancing NLO properties involves modifying molecular structures, such as extending conjugation or incorporating additional electronic systems. Transition metal-based organometallic complexes are particularly valued for their redox properties, allowing for flexible NLO responses through charge transfer transitions without altering the ligand's oxidation state.

Thiourea-based transition metal complexes show promise for nonlinear optical (NLO) applications due to their unique properties. The sulfur atoms in thiourea form stable coordination bonds with transition metals, enhancing optical characteristics. This interaction leads to improved electronic structures, resulting in strong NLO responses, such as second harmonic generation

(SHG). These complexes also offer high thermal stability, crucial for practical NLO devices. Thiourea's versatility, combined with tunable metal centers, enables the development of materials for various optoelectronic applications. They have also been extensively studied for their industrial and biological applications such as antibacterial and anticancer [1]. The sulphur-containing functional group in thiourea provides diverse bonding opportunities, making it a versatile ligand in coordination chemistry [2]. Intermolecular hydrogen bonds between sulphur and hydrogen atoms enhance the stability of crystal structures and dimer formation [3]. Synthesis of the complexes by reacting thiourea with metal salts combines organic and inorganic components. Techniques like IR spectroscopy, NMR, and UV-Vis offer detailed insights into their structures. For NLO applications, the optical properties of thiourea metal complexes are influenced by the choice of metal ion. Computational chemistry, especially Density Functional Theory (DFT), aids in designing and predicting NLO properties efficiently. DFT, using the B3LYP method and 6-31G(d,p) basis set, optimizes molecular structures and calculates frontier molecular orbital energies, providing comprehensive characterization of these complexes [4].

The synthesis of thiourea can be accomplished through various methods, with conventional reflux and microwave irradiation being two notable techniques. The process involves the reaction between 2-naphthylamine with 1-naphthyl isothiocyanate in dichloromethane under reflux conditions, followed by filtration and washing with ethanol to isolate the product. Microwave irradiation offers several advantages over traditional heating methods, as noted by [5]. It drastically reduces reaction times from hours to minutes, increases the product yields. These advantages make microwave-assisted synthesis an attractive alternative in chemical reactions, promising greater efficiency and productivity in laboratory environments. Thiourea exhibits a strong affinity for metal ions, making it an effective ligand for the synthesis of metal complexes. The sulfur atoms in thiourea can form strong coordination bonds with various metal ions, including transition metals. This strong metal-binding ability ensures the stability and integrity of the metal complex [6]. The complexes formed by thiourea with different metals, such as heterocyclic compounds, display biological activity [7]. As thiourea is commonly used in the pharmaceutical industry, its choice as a ligand is well-accepted. Complexes of cobalt (Co), nickel (Ni), zinc (Zn), and palladium (Pd) have generated particular interest in bioinorganic applications due to their ability to bind human proteins [8]. Several methods for producing metal complexes have been reported. One approach involves reacting thiourea ligands (L) with  $\text{CoCl}_2$ ,  $\text{NiBr}_2$ ,  $\text{PdX}_2$  ( $\text{X} = \text{Cl}; \text{Br}$ ), and  $\text{ZnI}_2$  in acetonitrile at room temperature to synthesize the corresponding four-coordinate monomeric  $[\text{L}_2\text{CoCl}_2]$ ,  $[\text{L}_2\text{NiBr}_2]$ ,  $[\text{L}_2\text{PdX}_2]$  ( $\text{X} = \text{Cl}$  or  $\text{Br}$ ), and  $[\text{L}_2\text{ZnI}_2]$  complexes [9].

Metal complexes containing thiourea ligands, particularly those involving copper, cadmium, and cobalt, have diverse applications due to their unique chemical and physical properties, with a strong emphasis on their nonlinear optical (NLO) characteristics. Copper-thiourea complexes are valuable in catalysis for organic transformations, antimicrobial activities, and electrochemical applications like sensors and electrocatalysts. Cadmium-thiourea complexes are known for their photoluminescence, making them useful in optoelectronics, heavy metal detection, and cancer therapeutics, with their NLO properties enhancing their role in photonics. Cobalt-thiourea complexes, with magnetic properties and applications in hydrogen and oxygen evolution reactions for renewable energy, also exhibit NLO properties and demonstrate antibacterial, antifungal, and anticancer activities. Overall, these complexes' NLO properties are integral to their impact on photonics, renewable energy, and medicinal chemistry [11].

This study investigates the synthesis and characterization of thiourea-based ligands and their metal complexes for nonlinear optical (NLO) applications, highlighting the use of thiourea's ability to form stable complexes with metal ions to enhance NLO responses. The reflux method is employed for efficient synthesis, addressing challenges in traditional techniques, while computational studies predict NLO properties to design tailored metal complexes. Transition metals like copper, cadmium, and cobalt, when coordinated with 1,3-diphenylthiourea, improve NLO properties due to their electronic transitions and varying oxidation states, which facilitate charge transfer, polarization effects, and enhance second- and third-order NLO effects, such as second-harmonic generation, making these complexes ideal for NLO applications [10].

## 2.0 EXPERIMENTAL

### 2.1 Materials

Aniline, Copper(II) chloride, Cobalt(II) chloride hexahydrate, Cadmium(II) chloride, Ethanol, Acetonitrile, Dichloromethane, Benzyl isothiocyanate, 98%.

### 2.2 Preparation of materials

The preparation began with the synthesis of the ligand, 1,3-diphenylthiourea. Followed by the formation of the complexes with different metals, specifically copper(II), cadmium(II), and cobalt(II). The structures of the metal-ligand complexes were characterized using different characterization techniques. Finally, the study investigates the nonlinear optical (NLO) properties of these metal-containing ligands through NLO calculations using Gaussian software.

## 2.2.1 Synthesis of Ligand

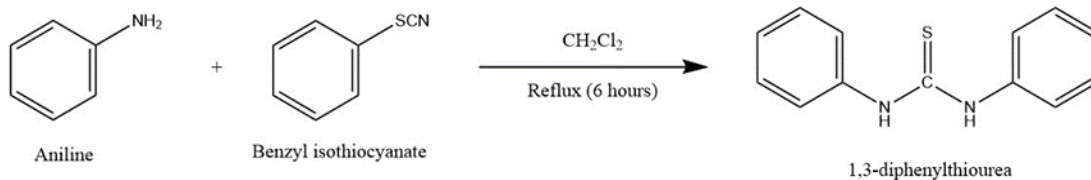


**Figure 1** Reaction scheme for ligand

Figure 1 depicts the synthesis of the ligand via the reflux method. Aniline (3.49 g) and 1-benzyl isothiocyanate (5.59 g) were mixed with dichloromethane and stirred. The mixture was refluxed for 6 hours, forming a white solid product. After filtration, the product was washed with dichloromethane, dried, and characterized using FTIR,  $^1\text{H}$  NMR, and UV-Vis spectroscopy to confirm its identity and purity.

## 2.3 Synthesis of Metal Complexes

### 2.3.1 Synthesis of Copper(II) Complex (CA)

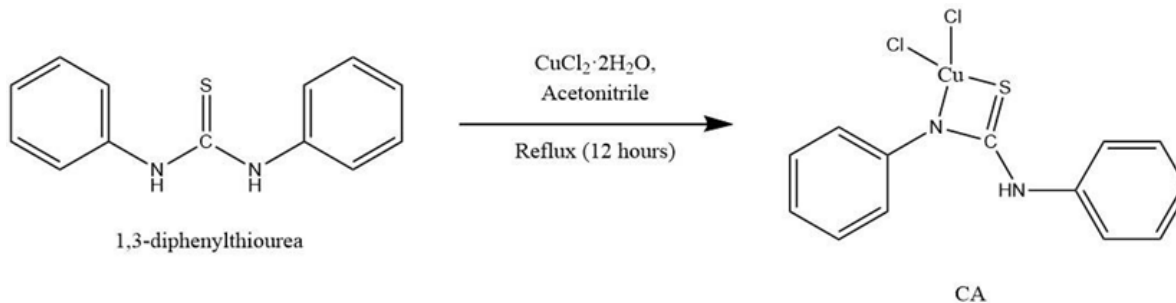


**Figure 2** Reaction scheme for CA

A solution of  $\text{CuCl}_2 \cdot 2\text{H}_2\text{O}$  (0.1072 g, 0.8 mmol) was prepared in acetonitrile (5 mL). The solution was refluxed with stirring for approximately 2 hours, followed by the dropwise addition of 1,3-diphenylthiourea (0.1826 g, 0.8 mmol) dissolved in acetonitrile (5 mL). The solution was then refluxed and stirred continuously for 12 hours at  $70^\circ\text{C}$ , resulting in a yellowish-coloured solution. The reaction mixture was filtered and left for slow evaporation at room temperature.

### 2.3.2 Synthesis of Cadmium(II) Complex (CB)

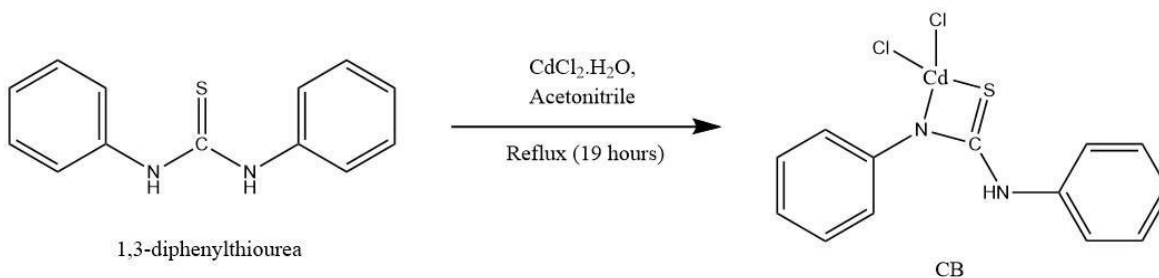


**Figure 3** Reaction scheme for CB

A solution of  $\text{CdCl}_2 \cdot \text{H}_2\text{O}$  (0.1611 g, 0.8 mmol) was prepared in acetonitrile (5 mL). The solution was refluxed with stirring for approximately 2 hours, followed by the dropwise addition of 1,3-diphenylthiourea (0.1826 g, 0.8 mmol) dissolved in acetonitrile (5 mL). The solution was refluxed and stirred continuously for 19 hours at  $70^\circ\text{C}$ , resulting in a cloudy solution. The reaction mixture was filtered and left for slow evaporation at room temperature.

### 2.3.3 Synthesis of Cobalt(II) Complex (CC)

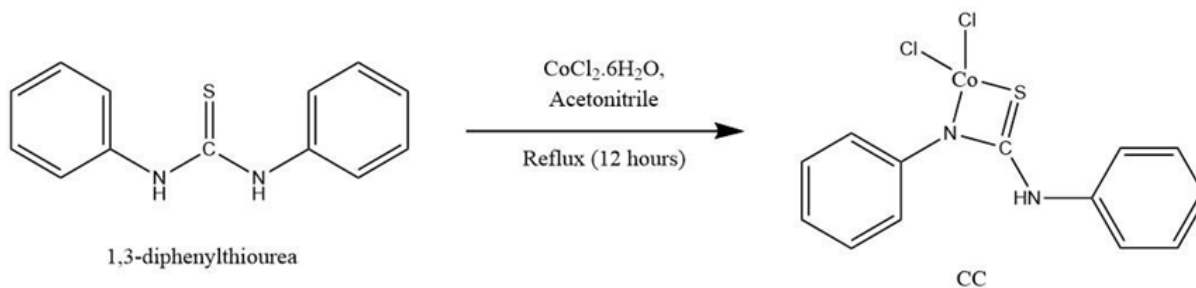


**Figure 4** Reaction scheme for CB

The reaction began by dissolving 0.1903 g (0.8 mmol) of cobalt chloride hexahydrate ( $\text{CoCl}_2 \cdot 6\text{H}_2\text{O}$ ) in 5 mL of acetonitrile, followed by refluxing with stirring for 2 hours to dissolve the cobalt salt. Then, 0.1826 g (0.8 mmol) of 1,3-diphenylthiourea, dissolved in 5 mL of acetonitrile, was added dropwise to the cobalt solution. The mixture was kept under reflux at  $70^\circ\text{C}$  for 12 hours, resulting in a blue solution of the complex. After reflux, the mixture was filtered to remove impurities, and the solution was left to evaporate at room temperature for crystallization. The resulting cobalt-thiourea complex was then further characterized.

### 2.4 Characterization of materials

The prepared metal complexes were characterized using various characterization methods to determine their structure and properties. These methods include FT-IR spectroscopy (PerkinElmer, model: 1600 series), UV-Vis spectroscopy (Shimadzu UV-1800 UV/Visible spectrophotometer), and NMR spectroscopy. The ligand and the three metal complexes (CA, CB, and CC) were found to be novel, indicating the need for further detailed characterization.

## 3.0 RESULTS AND DISCUSSION

### 3.1 Synthesis of Ligand

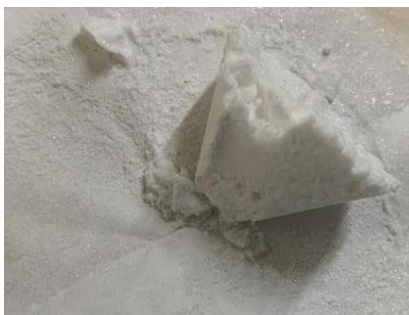


**Figure 5** Ligand

Yield (6.60 g, 77.05 %), white powder. IR (ATR):  $3360.85 \text{ m } \nu(\text{N-H})$ ,  $1242.98 \text{ s } \nu(\text{C=S})$ ,  $3137.76 \text{ m } \nu(\text{C=C})$ .  $^1\text{H NMR}$  (DMSO/ppm):  $\delta$  9.633 (H,  $\text{NH}_a$ ),  $\delta$  8.169 (H,  $\text{NH}_b$ ),  $\delta$  7.095-7.427 (CH-Ar).

## 3.2 Synthesis of Metal Complexes

### 3.2.1 Synthesis of Copper(II) Complex (CA)



**Figure 6** CA

Appearance: Brownish green solid. IR (ATR): 3303.75 m  $\nu$ (N-H), 846.93 s  $\nu$ (C=S), 1470.72 m  $\nu$ (C=C).  $^1\text{H}$  NMR ( $\text{CHCl}_3/\text{ppm}$ ):  $\delta$  8.621 (H,  $\text{NH}_a$ ),  $\delta$  7.402 (H,  $\text{NH}_b$ ),  $\delta$  6.652-7.367 (CH-Ar).

### 3.2.2 Synthesis of Cadmium(II) Complex (CB)



**Figure 7** CB

Appearance: White solid. IR (ATR): 3208.89 m  $\nu$ (N-H), 1350.52 s  $\nu$ (C=S), 1470.72 m  $\nu$ (C=C).

### 3.2.3 Synthesis of Cobalt(II) Complex (CC)



**Figure 8** CC

Appearance: Brick red solid. IR (ATR): 3208.89 m  $\nu$ (N-H), 1350.52 s  $\nu$ (C=S), 1470.72 m  $\nu$ (C=C).

### 3.2.4 Geometry Optimization using DFT Method

**Table 1** Optimized energy (a.u.) and dipole moment (D) obtained from the optimized studied compounds.

Compound	Energy (a.u.)	Dipole Moment (D)
Ligand	-1010.15	5.744656
CA	-2126.78	13.099192
CB	-1978.72	12.882459
CC	-1185.41	11.630768

The results showed that the molecular energy of the complexes is higher than that of the ligand, due to the presence of copper, cadmium and cobalt metal centers, which stabilize the complexes by forming back donation interactions with the ligand. The molecular energy of CA (-2126.78 a.u.) was the highest after optimization, followed by CB (-1978.72 a.u.), CC (-1185.41 a.u.) and the ligand (-1010.15 a.u.). Typically, a compound with a greater number of atoms will have higher energy compared to a compound with fewer atoms.

## 3.3 Characterization

### 3.3.1 Infrared Spectroscopy

Information about the functional group's stretching or bending frequencies, resulting from bond vibrations, is obtained through characterization using FT-IR spectroscopy. The calculated data for the ligand and complexes were derived from the DFT/B3LYP/6-31G(d,p) and DFT/B3LYP/GEN methods, respectively. The FT-IR spectrum of the ligand shows a C=S stretching peak at 1242.98  $\text{cm}^{-1}$  (experimental) and 1200.34  $\text{cm}^{-1}$  (computational), indicating the formation of the ligand. Upon complexation, the experimental value for C=S stretching of CA, CB and CC were 1028.01  $\text{cm}^{-1}$ , 1183.81  $\text{cm}^{-1}$  and 1205.50  $\text{cm}^{-1}$ , respectively. Additionally, the computational data for the same stretching appears at 1035.74  $\text{cm}^{-1}$  (CA), 1196.70  $\text{cm}^{-1}$  (CB) and 1221.18  $\text{cm}^{-1}$  (CC). Percentage deviations, calculated between experimental and computational results, are shown in Table 2. The deviations are less than 5%, indicating that the method is reliable.

**Table 2** Summarized data of FT-IR spectroscopy for Ligand, CA, CB, and CC.

Compounds	Mode	NH ( $\text{cm}^{-1}$ )	C=S ( $\text{cm}^{-1}$ )	C-H ( $\text{cm}^{-1}$ )	C-N ( $\text{cm}^{-1}$ )
<b>Ligand</b>	Experimental	1535.98	1242.98	3137.76	1350.39
	Computational	1562.31	1200.34	3178.65	1350.56
	% Deviation	1.71	3.43	1.30	0.01
<b>CA</b>	Experimental	1628.86	1028.01	3029.31	1177.19
	Computational	1623.50	1035.74	3186.75	1194.89
	% Deviation	0.33	0.75	5.40	1.50
<b>CB</b>	Experimental	1593.52	1183.81	3059.67	1298.18
	Computational	1572.59	1196.70	3063.48	1291.79
	% Deviation	1.28	1.08	0.12	0.49
<b>CC</b>	Experimental	1592.95	1205.50	3141.96	1296.34
	Computational	1603.31	1221.18	3188.20	1310.81
	% Deviation	0.65	1.30	1.47	1.11



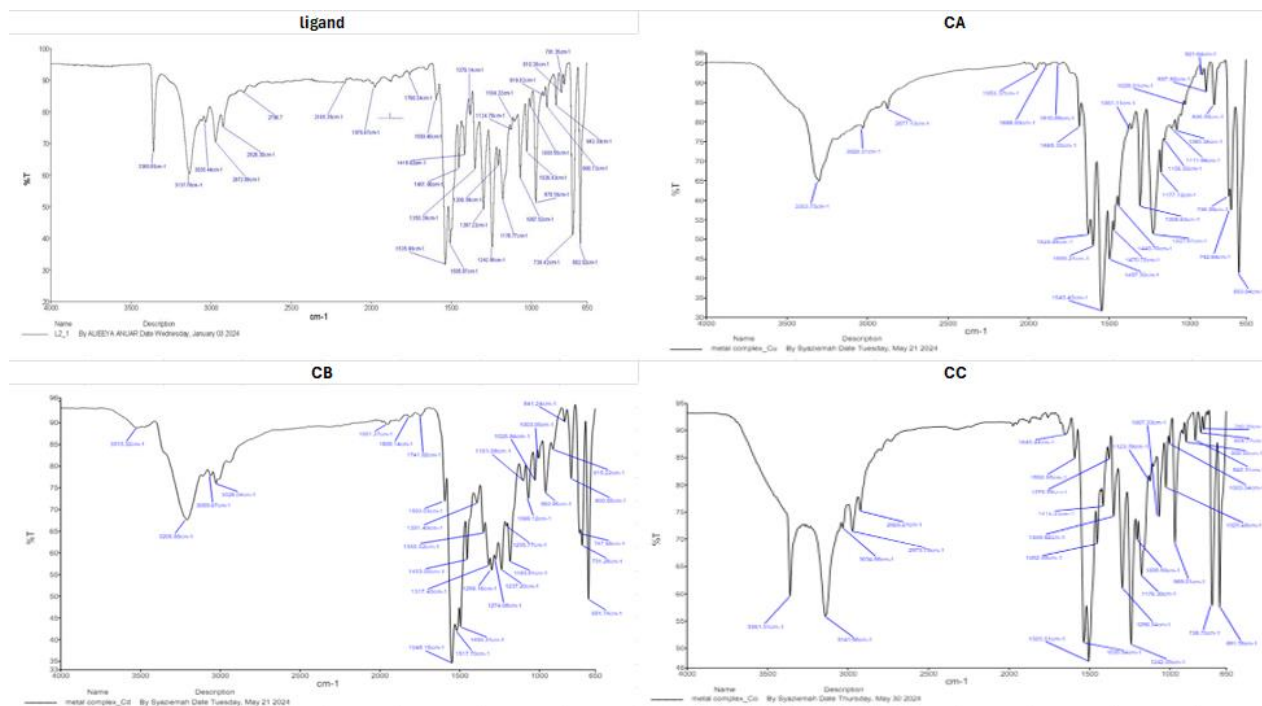


**Figure 9** FT-IR spectrum for the Ligand, CA, CB and CC plotting % Transmittance vs Wavenumbers (cm<sup>-1</sup>).

### 3.3.2 <sup>1</sup>H NMR spectroscopy

The relative ionic species can be identified using the NMR isotropic chemical shift analysis, which allows for the computation of reliable magnetic properties to predict the molecular geometry and the number of protons in the molecular structure. The studied compounds were analyzed using this method in dimethyl sulfoxide (DMSO) at 400 MHz. The DFT/B3LYP/GEN and DFT/B3LYP/6-31G methods were employed to compute the calculated data for the optimized ligands and complexes. For <sup>1</sup>H NMR, the computation was based on the GIAO method. The chemical shift ( $\delta$ ) of the compounds were reported in ppm relative to the <sup>1</sup>H NMR spectra. The computational calculations were performed in the gas phase, in which the value might be different as the experimental value was done in the solvent phase.

In general, the main chemical shift observed in this spectrum corresponds to the proton attached to the amine group (C-N-H). The peak is expected to appear around  $\delta$  8 ppm (a downfield region), due to the presence of nitrogen atom, which acts as an electronegative atom, causing the peak to be more deshielded. Additionally, protons in aromatic ring are expected to appear in the range of 6 – 8 ppm due to the conjugation effects along the benzene ring. The  $\pi$ -bonding electron in the benzene ring acts as a conductor, causing the protons to become more deshielded and shift to the downfield region, resulting in a higher chemical shift.

The <sup>1</sup>H NMR results of the ligand, using DMSO as a solvent, showed a chemical shift for the amine group (C-N-H) at  $\delta$  8.8 ppm and for the aromatic protons (Ar-H) between  $\delta$  6.4 and 7.7 ppm. The nitrogen atom in the amine group deshielded the proton, shifting it downfield. DFT calculations support the experimental data, showing a chemical shift for the amine group at  $\delta$  9.633 ppm, with a 29.5% deviation, and for the aromatic protons between  $\delta$  5.2929 and 8.0527 ppm. In the complex, the amine proton shifts downfield to  $\delta$  8.621 ppm, indicating ligand coordination to the copper metal, which further deshielded the proton. The aromatic protons also shift downfield due to the influence of copper and the electron-donating chlorine group, with a shift from  $\delta$  7.095-7.427 ppm in the ligand to  $\delta$  6.652-7.367 ppm in the complex. DFT calculations show a shift for the complex between  $\delta$  5.387 and 6.9762 ppm. The experimental and calculated data, summarized in Table 3, reveal that the solvation effect must be considered when comparing both datasets, as computational values may differ slightly from experimental results. The accuracy of the data depends on the percentage deviation, which should ideally be less than 5%.

**Table 3** Summarized data of <sup>1</sup>H NMR spectroscopy for Ligand, CA, CB, and CC.

Compound	Mode	NH (A)	NH (B)	H-Ar
Ligand	Experimental (ppm)	9.633	8.169	7.095-7.427
	Computational (ppm)	6.008	5.7565	5.2929-8.0527
	% deviation	37.6	29.5	-
CA	Experimental (ppm)	8.621	7.402	6.652-7.367
	Computational (ppm)	7.017	6.0595	5.387-6.9762
	% deviation	18.6	18.1	-
CB	Experimental (ppm)	9.778	7.409	6.365-7.390
	Computational (ppm)	7.1941	5.7743	6.4267-6.8986
	% deviation	26.4	22.1	-
CC	Experimental (ppm)	7.496	7.114	6.934-7.068
	Computational (ppm)	8.3679	6.3095	5.8291-7.0766

### 3.3.3 UV-Vis Spectroscopy

UV-Vis spectroscopy provides insight into the Metal-to-Ligand Charge Transfer (MLCT) and Ligand-to-Metal Charge Transfer (LMCT) processes between transition metals and thiourea ligand. The calculations were performed using the TDDFT/B3LYP/6-31G(d,p) method with a set number of cycles, N=7 in a gas phase. In each cycle, electrons transition from a lower state to a higher excited state. As the number of cycles increases, multiple calculations are executed, leading to a greater number of excited states being considered, thereby enhancing the accuracy of the absorption data. Additionally, TD-DFT was utilized for Frontier Molecular Orbital (FMO) analysis and UV-Vis spectral analysis.

The electronic absorption spectra of the compounds were measured within the wavelength range of 200-800 nm. For the experimental setup, the ligand was dissolved in DCM at a concentration of  $1 \times 10^{-12}$  M, while the complexes were dissolved in chloroform at a concentration of  $1 \times 10^{-9}$  M.

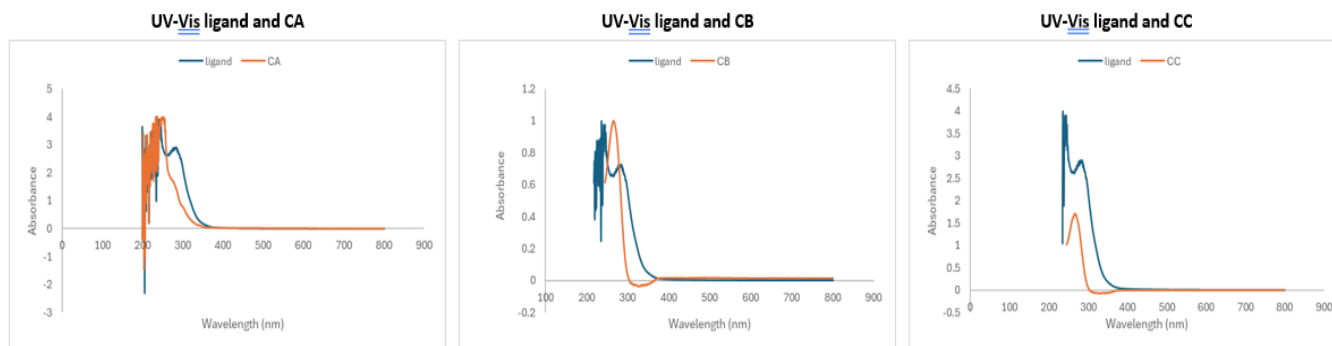
Table 4 presents the UV-Vis absorption data for the ligand and its corresponding complexes, providing valuable information about the maximum absorption wavelengths, absorbance, and oscillator strengths. For the ligand, the experimental  $\pi \rightarrow \pi^*$  transition is observed at 238 nm, which shifts upon complexation. In compound CA, this transition moves to 253 nm, with an additional MLCT transition observed at 701 nm. In compound CB, the  $\pi \rightarrow \pi^*$  transition shifts to 266 nm, and the MLCT transition appears at 429 nm. Similarly, in compound CC, the transition shifts to 265 nm, and the MLCT transition is observed at 507 nm. These shifts in the  $\pi \rightarrow \pi^*$  absorption maxima and the appearance of MLCT transitions strongly suggest the successful coordination of the ligand with the metal center. The increase in the MLCT absorption bands further supports the notion of complex formation.

Additionally, the oscillator strength (f), which is a key indicator of the intensity of electronic transitions, tends to be higher in compounds with enhanced nonlinear optical (NLO) properties. In this dataset, the ligand itself shows a higher oscillator strength, indicating its potential for significant NLO activity. This is consistent with the computational data, where the ligand also exhibits a higher oscillator strength, although the values between the experimental and theoretical data differ. The discrepancy in oscillator strength values may arise from solvent effects or the different conditions under which the experimental and computational measurements were taken. Nonetheless, the UV-Vis spectroscopy results provide crucial evidence for the successful complexation of the ligand with the metal centers and underscore the ligand's potential for NLO applications.



**Table 4** Comparison of absorption band of studied compound

Compound	Mode	$\lambda_{\max}$ (nm)	Abs./ Oscillator Strength, f
Ligand	Experimental	238.00	4.0
	Computational	277.68	0.3635
CA	Experimental	253.00, 701.00	3.887, 0.008
	Computational	868.63	0.0561
CB	Experimental	266, 429	1.170, 0.020
	Computational	342.61	0.0503
CC	Experimental	265, 507	1.689, 0.003
	Computational	1321.16	0.0034

**Figure 10** UV-Vis spectrum of the ligand, CA, CB, and CC, plotting absorbance vs wavelength.

### 3.3.4 NLO Calculations

The complexes selected for the NLO calculations were chosen based on their optimized geometries using the Density Functional Theory (DFT) approach. This method is known to provide highly accurate geometric structures by accounting for both bond lengths and bond angles. Generally, increasing the size of the basis set improves the accuracy of the calculations, reducing errors in bond length predictions. Furthermore, the use of hybrid DFT, specifically the B3LYP functional, allows for more precise geometric structures by including electron correlation, making it especially reliable for larger systems or complexes involving transition metals.

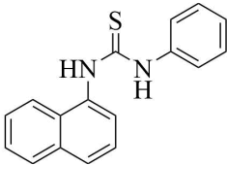
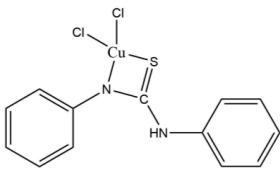
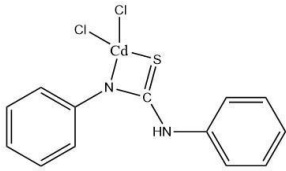
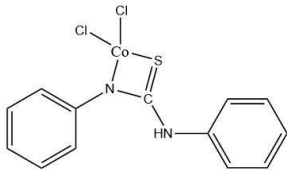
When transition metals such as copper, cadmium, and cobalt are combined with ligands containing electron-donating or withdrawing groups, as well as distinct conjugated systems, the resulting electronic structures and charge transfer properties are significantly altered. These changes directly affect the nonlinear optical (NLO) properties of the complexes. To assess these properties, key parameters such as the dipole moment and the HOMO-LUMO energy gap can be used to evaluate the total first-order hyperpolarizability ( $\beta_{\text{tot}}$ ), which serves as an indicator of the second-order NLO characteristics. Table 5 summarizes the frequency-dependent first hyperpolarizability values, which were derived from  $\beta(-2\omega; \omega, \omega)$  based on second harmonic generation (SHG) calculations at a wavelength of 1064 nm.

The results clearly showed that the CC complex exhibits the highest  $\beta_{\text{tot}}$  value of  $6030.985 \times 10^{-30}$  esu, followed by the CA complex with a  $\beta_{\text{tot}}$  of  $919.9551 \times 10^{-30}$  esu, and the CB complex with the lowest  $\beta_{\text{tot}}$  of  $294.4103 \times 10^{-30}$  esu. These findings indicate that the CC complex proved to be the strongest NLO material, suggesting its potential as an excellent candidate for NLO applications, while the CB complex showed comparatively weaker NLO behavior.

Table 5 also illustrates the relationship between energy gap, dipole moment and first order hyperpolarizability,  $\beta_{\text{tot}}$  obtained. On one hand, CA is computationally expected to exhibit a better NLO response compared to CB and CC. This is in the reference

of dipole moment of CA being higher than CB and CC. However, the relationship between the band gap and NLO response is contradictory, as CB possesses a higher band gap (0.09517 eV) compared to CA (0.00457 eV) and CC (0.03461 eV). Due to the small difference in the band gap values (0.06 eV), it can be concluded that the band gap is similar across all complexes.

**Table 5** Comparison between band gap, dipole moment and  $\beta_{\text{tot}}$  values for Ligand, CA, CB and CC.

Compound	Band Gap (eV)	Dipole moment (D)	$\beta_{\text{tot}}$ ( $\times 10^{-30}$ esu)
 Ligand	0.09451	5.744656	343.4845
 CA	0.00457	13.099192	919.9551
 CB	0.09517	12.882459	294.4103
 CC	0.03461	11.630768	6030.985

#### 4.0 CONCLUSION

The study successfully achieved its objectives by synthesizing and characterizing ligands and their complexes with copper, cadmium, and cobalt using both experimental and computational methods, specifically Density Functional Theory (DFT). The developed compounds exhibited structural and electronic properties that were consistent with theoretical predictions, with deviations below 5%. Functional groups such as -C-N, C=C aromatic, and C-H aromatic were confirmed in the complexes, indicating coordination between the metals and ligands. Shifts in proton resonance further supported the metal-ligand interactions. UV-vis spectroscopy confirmed these interactions, showing wavelength shifts in the spectra of the metal complexes. Additionally, DFT calculations were employed to study the nonlinear optical (NLO) properties of ligands with different metals, including geometry optimizations for all the studied compounds.

The results reveal that the CC (cobalt) complex exhibits the highest total first-order hyperpolarizability ( $\beta_{\text{tot}}$ ) of 6030.985  $\times 10^{-30}$  esu, followed by the CA (copper) complex at 919.9551  $\times 10^{-30}$  esu, and the CB (cadmium) complex at 294.4103  $\times 10^{-30}$  esu, indicating that the CC complex has the strongest NLO properties. While copper has a smaller HOMO-LUMO gap, which typically suggests better electronic excitation, NLO properties depend on more than just this gap. The superior NLO performance

of the cobalt complex is likely due to its optimal metal-ligand interaction, charge delocalization, and coordination environment around the cobalt ion, which enhances polarization and improves the efficiency of nonlinear processes. The copper complex, despite its smaller HOMO-LUMO gap, may not exhibit as strong NLO behavior due to less efficient charge transfer, while cadmium's NLO properties are weaker because to its less favorable electronic structure. Therefore, the cobalt complex emerges as the best candidate for NLO applications due to its combination of favorable electronic structure, metal-ligand interactions, and charge transfer capabilities.

## Acknowledgment

The researchers would like to acknowledge the research grant support from the Ministry of Higher Education, Malaysia for the Fundamental Research Grant Scheme (FRGS/1/2021/STG04/UTM/02/7). Faculty of Science UTM, and the Centre for Information and Communication Technology (CICT) for supporting and providing high-performance computing facilities and services that expedited the research. Thank you to the colleagues for the valuable support and suggestions.

## References

- [1] Mishra, A., Ninama, S., Sharma, P., Soni, N., & Awate, R. (2012). A newly synthesis and characterization of metal complexes of 3-(N-phenyl) thiourea-pentanone-2 as ligand. *Journal of Physics: Conference Series*, 365(1), Article 012039. <https://doi.org/10.1088/1742-6596/365/1/012039>
- [2] Daami, N., & Ali, R. (2015). Synthesis and characterization of 1-(4-chloro phenyl)-3-(pyrimidin-2-yl) thiourea and its complexes with cobalt(II), nickel(II), and copper(II). *International Journal of Scientific and Engineering Research*, 7(5), 87–93. <https://www.iiste.org>
- [3] Binzet, G., Kavak, G., Külcü, N., Özbey, S., Flörke, U., & Arslan, H. (2013). Synthesis and characterization of novel thiourea derivatives and their nickel and copper complexes. *Journal of Chemistry*, 2013, Article 536562. <https://doi.org/10.1155/2013/536562>
- [4] Raza, M. A., Javaid, K., Farwa, U., Javaid, A., Yaseen, M., Maurin, J. K., Budzianowski, A., Iqbal, B., & Ibrahim, S. (2023). One pot efficient synthesis of 1,3-di (naphthalen-1-yl) thiourea: X-ray structure, Hirshfeld surface analysis, density functional theory, molecular docking, and in-vitro biological assessment. *Journal of Molecular Structure*, 1271, Article 133989. <https://doi.org/10.1016/j.molstruc.2022.133989>
- [5] Sapari, S., Zakariah, E. I., Razak, N. H. A., Ramzan, I., Numin, M. S., Heng, L. Y., & Hasbullah, S. A. (2021). A comparative study of microwave-assisted and conventional heating methods for the synthesis of 1-(naphthalene-1-yl)-3-(o, m, p-tolyl)thioureas, DFT analysis, antibacterial evaluation, and drug-likeness assessment. *Sains Malaysiana*, 50(3), 743–751. <https://doi.org/10.17576/jsm-2021-5003-16>
- [6] Al-Halbosy, A. T. F., Hamada, A. A., Faihan, A. S., Saleh, A. M., Yousef, T. A., Abou-Krishna, M. M., Alhalafi, M. H., & Al-Janabi, A. S. M. (2023). Thiourea derivative metal complexes: Spectroscopic, anti-microbial evaluation, ADMET, toxicity, and molecular docking studies. *Inorganics*, 11(10), Article 390. <https://doi.org/10.3390/inorganics11100390>
- [7] Javadzade, T., Rzyayeva, I., Demukhamedova, S., Akverdieva, G., Farzaliyev, V., Sujayev, A., & Chiragov, F. (2023). Synthesis, structural analysis, DFT study, antioxidant activity of metal complexes of N-substituted thiourea. *Polyhedron*, 231, Article 116274. <https://doi.org/10.1016/j.poly.2022.116274>
- [8] Noor, A., Qayyum, S., Ali, Z., & Muhammad, N. (2023). Syntheses and structural characterization of divalent metal complexes (Co, Ni, Pd, and Zn) of sterically hindered thiourea ligand and a theoretical insight into their interaction with SARS-CoV-2 enzyme. *Journal of Molecular Structure*, 1274(2), 42–54. <https://doi.org/10.1016/j.molstruc.2022.134>
- [9] Lewars, E. G. (2016). An outline of what computational chemistry is all about. In *Computational chemistry* (2nd ed., pp. 1–50). Springer. <https://doi.org/10.1007/978-3-319-30685-6>
- [10] Farooq, S., Hussain, A., Yar, M., Tariq, M., Mahmood, K., Ayub, K., Hussain, R., Rasool, F., Imran, M., & Assiri, M. A. (2023). Nonlinear optical response of facially polarized all cis-1,3,5-trifluorocyclohexane doped with transition metals and calcium. *Journal of Molecular Liquids*, 391, Article 123331. <https://doi.org/10.1016/j.molliq.2023.123331>
- [11] Canudo-Barreras, G., Ortego, L., Izaga, A., Marzo, I., Herrera, R. P., & Gimeno, M. C. (2021). Synthesis of new thiourea-metal complexes with promising anticancer properties. *Molecules*, 26(22), Article 6891. <https://doi.org/10.3390/molecules26226891>